

Characterization and catalytic properties of Ni–Sn intermetallic compounds in acetylene hydrogenation

Ayumu Onda, Takayuki Komatsu* and Tatsuaki Yashima

Department of Chemistry, Tokyo Institute of Technology, 2-12-1 Ookayama, Meguro-ku, Tokyo, 152-8550, Japan. E-mail: komatsu@chem.titech.ac.jp

Received 21st February 2000, Accepted 8th May 2000

Published on the Web 12th June 2000

The surface and catalytic properties of Ni–Sn intermetallic compounds (IMCs), Ni₃Sn, Ni₃Sn₂ and Ni₃Sn₄, were studied by X-ray photoelectron spectroscopy (XPS), temperature programmed reduction (TPR) and catalytic reactions, such as the hydrogenation of acetylene, H₂–D₂ equilibration and H–D exchange between C₂D₄ and H₂. The XPS results clarified that nickel and tin atoms near the surface were reduced into Ni⁰ and Sn⁰ by the hydrogen treatment at 873 K. The surface of each Ni–Sn IMC had specific nickel compositions and Ni3d valence band spectra. The TPR results showed that each Ni–Sn IMC had a different peak temperature from pure nickel and each other. These results revealed that Ni–Sn IMCs had the genuine surface of each IMC phase. Ni₃Sn and Ni₃Sn₂ catalysts showed the high selectivity for the partial hydrogenation of acetylene into ethylene and did not catalyze the ethane formation. The high selectivity of Ni–Sn IMCs resulted from the very low activity of Ni₃Sn and inactivity of Ni₃Sn₂ for the ethylene hydrogenation. The H–D exchange between deuterized ethylene and hydrogen, however, proceeded even over Ni₃Sn₂. The cause of the low activity of Ni–Sn IMC for the ethylene hydrogenation was discussed in view of the reaction mechanism.

1. Introduction

Intermetallic compounds (IMCs) are known to be the compounds between two or more metal elements having simple stoichiometry. The most characteristic feature of IMCs is that their specific crystal structure is different from that of their component metals, while normal alloys have the same crystal structure as that of either component metal. The specific structure sometimes gives them unique bulk properties, such as shape memory effect, hydrogen storage ability, superconductivity, and so on. The surface properties of IMCs, however, have not attracted much attention from scientists. In addition to the specific structure, the combination of two elements, which are greatly different in the physicochemical nature, may generate unique catalytic properties.

In view of the catalysis, most of the investigations on IMC have dealt with so-called hydrogen storage alloys¹ because of their unique activity for hydrogen dissociation and the possibility for the stored hydrogen to participate in the reactions. Examples are the reports on LaNi₅^{2,3} and CeM₂ (M = Ru, Co, and Fe)⁴ for the synthesis of ammonia and for the hydrogenation of ethylene, LaCu₅⁵ for the synthesis of methanol, ThNi₅⁶ and CeAl₂⁷ for the methanation of CO, LaCu₂⁸ for the decomposition of 4-methyl-2-pentanol, TiFe⁹ for the hydrogenation of CO, and ZrPd₃ and CePd₃ for the hydrogenation of 1,3-butadiene.¹⁰ The elements, such as La, Ti, Zr and Ce, are easily transferred into the oxides and hydroxides. The surface of the above IMCs could not be the genuine surface with the specific structure of IMCs. In the case of LaNi₅, the surface has been reported to be covered with layers of La₂O₃ or La(OH)₃ and Ni particles. The surface was estimated to be similar to Ni metallic particles supported on La₂O₃ or La(OH)₃.¹¹ On the contrary, we expected that the genuine surface of IMCs would provide further unique catalytic properties.

Supported bimetallic catalysts have been studied to enhance the activity, selectivity and stability of their parent monometallic catalysts.¹² In some reports on conventional bimetallic catalysts, two kinds of metals have been reported to form IMCs.^{13–15} A typical example of such conventional bimetallic catalysts is Pt–Sn supported on alumina or silica, which is known to be a good catalyst for hydrocarbon reforming. In this catalyst system, Pt–Sn IMCs, such as PtSn₄, PtSn and Pt₂Sn, have been proposed to be the active species from the observation by TEM and EDX.¹⁶ Dautzenberg *et al.*¹⁷ have detected PtSn on silica after H₂ reduction at 623 K for 3 h, while it was detected on alumina only after the reduction at 923 K for 100 h. Masai *et al.*^{18,19} have reported that some kinds of IMCs, such as Ni₃Sn₂, Ni₃Sn₄ and NiSn, exist in Ni–Sn/SiO₂ catalyst. The apparent catalytic properties of bimetallic systems would mainly depend on the active species with the highest activity and/or the largest content. However, many kinds of IMCs are expected to have unique catalytic properties which have never been observed in the studies of the conventional bimetallic catalysts even with the same combination of element metals.

To clarify the catalytic properties of bulk IMCs would raise the possibility of obtaining new catalyst systems as well as providing some information on the active species in the conventional bimetallic catalysts. Verbeek and Sachtler²⁰ have studied pure platinum and Pt–Sn IMC (Pt₃Sn, PtSn and PtSn₂) powders by chemisorption of CO, ethylene and deuterium and reported that the surface is significantly rich in tin and that the desorption temperature becomes progressively lower with an increase in the proportion of tin. However, the catalytic properties of these IMCs have not been clarified satisfactorily. Recently the specific adsorptive and catalytic properties on certain surface alloys, such as Au–Ni(111)²¹ and Sn–Pt(111),^{22,23} were reported, with stable, designed and ordered surface structures. Preparation of the surface alloys

was achieved by the deposition of gold and tin onto Ni(111) and Pt(111), respectively.

We have already reported on the catalytic properties of bulk Co–Ge IMCs for the hydrogenation of acetylene²⁴ and bulk Pt–Ge IMCs for the hydrogenation of 1,3-butadiene.²⁵ These compounds gave a lower activity than the pure component metal, cobalt or platinum, for both hydrogenation and H₂–D₂ equilibration. However, Co–Ge IMCs catalyzed the hydrogenation of acetylene with the high selectivity to ethylene, while pure cobalt produced almost exclusively ethane. Pt–Ge IMCs showed a high selectivity for the partial hydrogenation of 1,3-butadiene into butenes. In this study, we took up bulk Ni–Sn intermetallic compounds to obtain further and general information on the catalytic properties of IMCs and to explore the capabilities of IMC catalysts. It is well known that nickel has a high activity for hydrogenation.²⁶ The Ni–Sn binary system is composed of three kinds of IMC, each with a different crystal structure such as Ni₃Sn, Ni₃Sn₂ and Ni₃Sn₄, according to the phase diagram.²⁷ Each IMC has a significant homogeneity range of the Ni/Sn ratio and keeps its structure over 1000 K, which means that the interaction between nickel and tin is strong enough to form highly stable IMCs. We carried out the hydrogenation of acetylene and ethylene, H₂–D₂ equilibration and H–D exchange between hydrogen and C₂D₄ over all kinds of Ni–Sn IMCs and pure nickel and will discuss their catalytic properties based on the results of characterizations, such as X-ray diffraction (XRD), X-ray photoelectron spectroscopy (XPS) and temperature programmed reduction (TPR).

2. Experimental section

2.1. Catalysts preparation

Ni–Sn intermetallic compounds (IMCs), Ni₃Sn, Ni₃Sn₂ and Ni₃Sn₄, were prepared by melting the mixture of nickel (Koch Chemicals, 99.99%) and tin (Soekawa Chemicals, 99.99%) powders in an alumina boat with an SiC electric furnace. The temperature was raised from room temperature to 1733 K for 5 h in flowing argon, which was passed through Mn/SiO₂ to remove oxygen and water. The temperature held for 8 h at 50 K lower temperature than the melting point of Ni₃Sn (1173 K), Ni₃Sn₂ (1483 K) and Ni₃Sn₄ (923 K). Then it was cooled gradually to room temperature in flowing argon. The resultant IMC ingots were crushed in air and filtered into fine powders with particle diameters of 25–38 μm. The powders of pure nickel and tin were also filtered to have the same range of diameters.

2.2. Characterization

The bulk structure of IMC powder was identified by powder X-ray diffraction (Rigaku, RINT 2400). The X-ray source was Cu K α at 40 kV and 100 mA. The reduction behavior of IMCs and pure nickel stored in air was examined by temperature programmed reduction (TPR). Under flowing H₂(5%)/N₂ gas mixture, the temperature of the catalyst bed was raised from room temperature to 873 K at a heating rate of 10 K min⁻¹ and the consumption of hydrogen was continuously measured by a TCD detector. The oxygen and water impurities in the H₂/N₂ gas mixture and water produced by the reduction of catalysts were removed by passing through the columns of OMI-I (Spelco) and P₂O₅ (Wako Pure Chemical Ind.), respectively.

XPS spectra of IMC and pure nickel were obtained by using ESCALAB 220i (Fisons Instruments) with an Al K α X-ray source. The sample, pressed into a pellet, was put into a pretreatment chamber. Before and after an *in situ* reduction treatment with a flowing H₂ (101 kPa) at 873 K for 1 h, the sample was transferred into the spectrometer *in vacuo* (below 10⁻⁷ Pa). The binding energy of 284.5 eV for C1s from surface

carbon contaminant was used for the binding energy calibration.

2.3. Catalytic reaction

A glass circulation system was used for the reduction of samples and subsequent catalytic reaction. For hydrogenation reactions, a mixture of acetylene and hydrogen or ethylene and hydrogen was circulated through the powdered catalyst. The partial pressures of acetylene, ethylene and hydrogen were 2.7 and 13 kPa, respectively. H₂–D₂ equilibration was performed with a mixture of H₂ (6.5 kPa) and D₂ (6.5 kPa) with or without acetylene (2.7 kPa) or ethylene (2.7 kPa). H–D exchange between C₂D₄ and H₂ was performed with a mixture of C₂D₄ (2.7 kPa) and H₂ (13 kPa). H₂ and D₂ were purified by passing through the Mn/SiO₂ column at room temperature and the silica gel column at 77 K. Acetylene and ethylene were purified by repeating a freeze–pump–thaw cycle. The gas composition was monitored with a gas chromatography and a quadrupole mass spectrometer (Ulvac, MASSMATE 100). Before each reaction, catalysts were reduced with circulating H₂ (27 kPa) at 873 K for 1 h.

3. Results and discussion

3.1. Characterizations

The bulk structures of Ni–Sn intermetallic compound (IMC) powders prepared with Ni/Sn atomic ratios of 3/1, 3/2 and 3/4 were analyzed by the powder X-ray diffraction (XRD). The XRD patterns, illustrated in Fig. 1, showed almost exclusively the peaks of Ni₃Sn, Ni₃Sn₂ and Ni₃Sn₄ phases, respectively. No diffraction peaks of component metals and the other IMCs were observed.

The surface of powdered IMC will be oxidized because IMC ingots were crushed and stored in air. We carried out temperature programmed reduction (TPR) to clarify the reduction behavior and determine the pretreatment conditions for catalytic reactions. As shown in Fig. 2, pure nickel (a), Ni₃Sn (b) and Ni₃Sn₂ (c) each gave a peak at 430, 445 and 470 K, respectively. Ni₃Sn₄ (d) gave three peaks at 475, 575 and 625 K. Ni₃Sn₄ has at least three kinds of oxidized sites on the surface before the reduction. The TPR profile of pure tin was not observed due to the low melting point of tin (505 K). We gained a TPR profile of silica supported tin particles with bulk structure of β -Sn phase prepared by chemical vapour deposition (CVD) of Sn(CH₃)₄, which showed a broad peak around 820 K. It is clear that Ni₃Sn₂, Ni₃Sn₂ and Ni₃Sn₄ did not give the peak at the same temperature as that of pure nickel and tin, which would indicate that clusters of pure

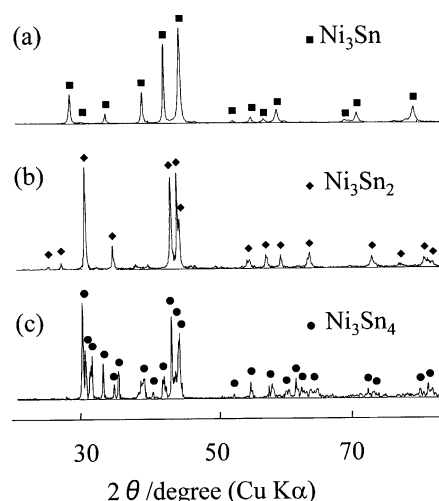


Fig. 1 X-ray diffraction patterns of Ni–Sn intermetallic compounds prepared with Ni/Sn atomic ratios of 3/1 (a), 3/2 (b) and 3/4 (c).

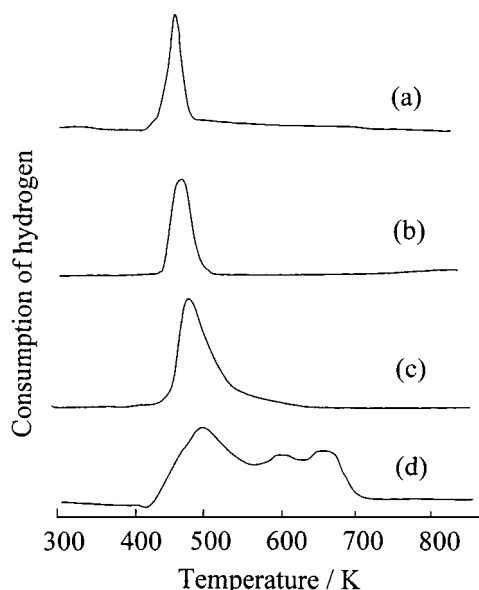


Fig. 2 TPR profiles of Ni(a), Ni₃Sn (b), Ni₃Sn₂ (c) and Ni₃Sn₄ (d).

nickel or tin do not exist on the surface. The TPR profiles of Ni–Sn IMCs were also different from each other, which implies that Ni₃Sn, Ni₃Sn₂ and Ni₃Sn₄ have each genuine surface. These results also indicated that the reduction of Ni–Sn IMC surface must be carried out at higher temperatures than 723 K to obtain the reduced surface.

The initial surface of Ni–Sn IMC powder just after crushing should be in a metallic state and have the genuine structure held by each crystal structure. However, TPR results revealed that the surface atoms were significantly oxidized in air. We studied the oxidation state of nickel and tin atoms near the surface by XPS. Table 1 shows XPS results of pure nickel and Ni–Sn IMCs before and after the reduction at 873 K with flowing hydrogen for 1 h. Pure nickel, before the reduction, gave two peaks derived from Ni2p_{3/2} at 852.8 and 856.6 eV. The peak at 852.8 eV would usually be attributed to Ni⁰. The peak at 852.8 eV might include Ni2p_{3/2} peaks of Ni²⁺ because Ni²⁺ gave three Ni2p_{3/2} peaks one of which appeared at about 853 eV in addition to about 856 eV.²⁸ After the reduction, it gave only Ni⁰ peak at 852.8 eV. Fig. 3 shows the Ni2p_{3/2} and Sn3d_{5/2} spectra of Ni₃Sn₂ before and after the reduction. Before reduction, Ni₃Sn₂ gave two Ni2p_{3/2} peaks at 852.8 eV of Ni⁰ (or Ni²⁺) and 856.4 eV of Ni²⁺ and two Sn3d_{5/2} peaks at 485.1 eV of Sn⁰ and 486.7 eV of Sn⁴⁺ (or Sn²⁺). After reduction, not only Ni2p_{3/2} but also Sn3d_{5/2} showed one peak from metallic atoms at 852.7 and 485.0 eV, respectively. This result indicates that the surface nickel and tin atoms were reduced into Ni⁰ and Sn⁰, respectively. In the cases of Ni₃Sn and Ni₃Sn₄, the oxidized nickel and tin were also reduced to Ni⁰ and Sn⁰ (Table 1). These results revealed

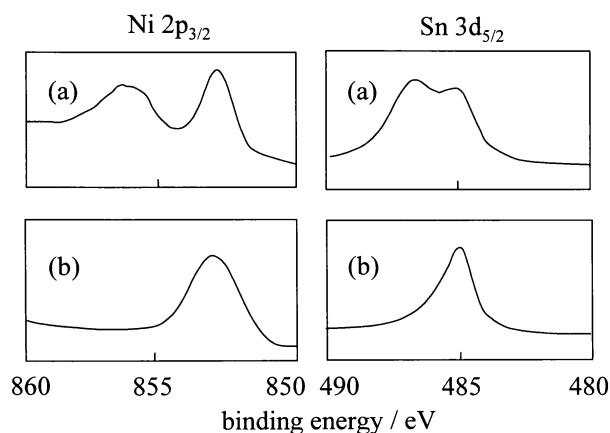


Fig. 3 XPS spectra of Ni 2p_{3/2} and Sn 3d_{5/2} in Ni₃Sn₂ before (a) and after (b) the H₂ reduction at 873 K for 1 h.

that all the surface atoms on Ni–Sn IMCs were reduced to the metallic state by the reduction with hydrogen at 873 K.

Table 1 also shows nickel compositions near surface and in the bulk expressed by Ni/(Ni + Sn) in atom%. The surface compositions were determined from the peak area of Ni2p_{3/2} and Sn3d_{5/2} XPS spectra by means of elemental sensitivity data of Wagner *et al.*,²⁹ The surface Ni composition increased with increasing the bulk one. However, the surface Ni composition was lower than the corresponding bulk one for all the Ni–Sn IMCs, which suggests relative enrichment in tin on the surface. Two reasons should be considered for this difference in the surface and bulk compositions. One reason is the presence of satellite peaks of Ni2p_{3/2}. The XPS peak of Ni2p_{3/2} is decomposed into some satellite peaks at higher binding energy in addition to its main peak at around 852.7 eV for metallic nickel.³⁰ Some of the satellite peaks would overlap with Ni2p_{1/2} peak at 870 eV and others would have higher binding energies. The actual surface Ni composition may be higher than the values in Table 1. The other reason is the difference in surface energy. Tin atoms should be comparatively stable on the top layer because the surface energy of tin is lower than that of nickel.^{31,32}

As shown in Table 1, little difference in the binding energies of Ni2p_{3/2} and Sn3d_{5/2} in Ni–Sn IMCs was observed from those in the pure metals. However, the influence of the IMC formation on nickel atoms was observed in their valence band as shown in Fig. 4. The peak near the Fermi level (binding energy of 0 eV) would be assigned to the Ni3d orbital because the lowest binding energy of tin is 25 eV of Sn4d.²⁸ Fig. 4 reveals the following changes with increasing tin content; the density of state at Fermi level decreased, the shape of Ni3d peaks narrowed, and the peak top of Ni3d shifted toward higher binding energy. These results also indicate that the genuine IMC surface would be formed on the surface of powdered Ni–Sn IMCs. The peak narrowing

Table 1 Results of XPS measurement

| Sample | | Binding energy/eV | | | Ni/(Ni + Sn) (atom%) | |
|---------------------------------|-------------------------|---------------------|------|---------------------|----------------------|-------------------|
| | | Ni2p _{3/2} | Ni3d | Sn3d _{5/2} | Surface ^a | Bulk ^b |
| Ni | Before rd. ^c | 852.8, 856.6 | N.d. | — | 100 | 100 |
| | After rd. ^d | 852.8 | 0.5 | — | 100 | 100 |
| Ni ₃ Sn | Before rd. | 852.6, 856.1 | N.d. | 485.0, 486.7 | N.d. | N.d. |
| | After rd. | 852.6 | 0.8 | 485.0 | 57 | 75 |
| Ni ₃ Sn ₂ | Before rd. | 852.8, 856.4 | N.d. | 485.1, 486.7 | N.d. | N.d. |
| | After rd. | 852.7 | 1.2 | 485.0 | 42 | 60 |
| Ni ₃ Sn ₄ | Before rd. | N.d. | N.d. | N.d. | N.d. | N.d. |
| | After rd. | 852.6 | 1.6 | 484.9 | 28 | 43 |
| Sn ⁰ (ref. 26) | | | | 485.0 | | |

^a Determined by XPS. ^b Calculated from the Ni/Sn ratio at the preparations. ^c Before reduction. ^d After reduction in hydrogen at 873 K for 1 h.

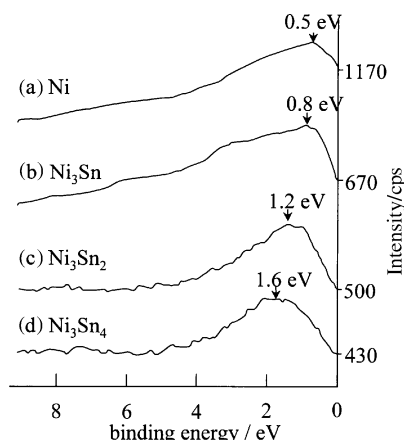


Fig. 4 Valence band XPS spectra after H_2 reduction at 873 K for 1 h.

would be due to the localization of free electrons. The shift toward higher binding energy would be due to the filling of the Ni3d orbital with electrons transferred from tin. These two changes could result in the decrease in the density of the state at the Fermi level. A similar peak shift has been reported for the valence band spectra of various IMCs, such as Ni–Al, Ni–Mg³³ and Pt–Ge.²⁵ In the case of the XPS spectrum of pure copper, the Cu3d peak is narrower and the binding energy at the peak top is higher than that of Ni3d.³⁴ Therefore, the Ni3d peak of Ni–Sn IMCs seemed to become closer to the Cu3d peak with increasing tin content, which also suggests some electron transfer from tin to nickel. This electron transfer would lead to the very negative heat of formation of Ni–Sn IMC. On the other hand, the Ni3d of Ni–Cu alloys was not different from that of pure nickel,³⁵ which means that the interaction between nickel and copper would be weak.

From the XRD, TPR and XPS studies, it is concluded that the surface of Ni_3Sn , Ni_3Sn_2 and Ni_3Sn_4 after the reduction does not include any clusters of nickel, tin and their oxides but has the genuine structure of each IMC. This conclusion made us expect that Ni_3Sn , Ni_3Sn_2 and Ni_3Sn_4 would show unique catalytic properties different from their component metals and each other.

3.2. Catalytic reactions

We studied the catalytic properties of Ni_3Sn , Ni_3Sn_2 and Ni_3Sn_4 for the acetylene hydrogenation compared with those of pure nickel. The powdered catalysts were reduced with hydrogen at 873 K for 1 h as a pretreatment. Fig. 5 shows the change in total pressure as a function of reaction time using the closed circulation system. The hydrogenation of acetylene leads to the decrease in total pressure. The reaction temperature was 373 K over nickel and 523 K over Ni_3Sn , Ni_3Sn_2 and Ni_3Sn_4 . Acetylene was not converted at 373 K over Ni–Sn IMCs. It is clear that the activity of Ni–Sn IMCs for acetylene hydrogenation was much lower than that of nickel. Particularly, Ni_3Sn_4 was almost inactive for the reac-

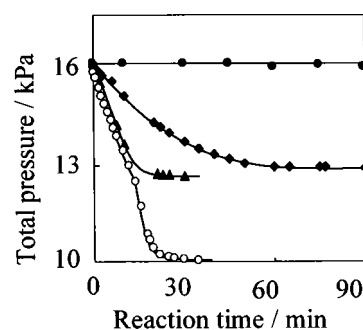


Fig. 5 The hydrogenation of acetylene on Ni (○, 0.30 g) at 373 K and Ni_3Sn (▲, 0.30 g), Ni_3Sn_2 (◆, 0.50 g) and Ni_3Sn_4 (●, 0.50 g) at 523 K. $P(H_2) = 13$ kPa, $P(C_2H_2) = 2.7$ kPa.

tion and showed very low activity even at 623 K. It is clear that the order of activity was as follows,

$$\text{nickel} \gg Ni_3Sn > Ni_3Sn_2 \gg Ni_3Sn_4 \approx 0.$$

Fig. 6 shows the change in the composition of gas phase hydrocarbon during acetylene hydrogenation over nickel (a), Ni_3Sn (b) and Ni_3Sn_2 (c) catalysts, respectively. Over pure nickel, the acetylene hydrogenation seemed to be a successive reaction. Acetylene was primarily hydrogenated into ethylene, followed by the secondary hydrogenation of ethylene into ethane. There may be also a reaction path in which acetylene is hydrogenated into ethane directly. Ethane was the main final product for acetylene hydrogenation over pure nickel.

Fig. 6b shows that ethylene was the main final product over Ni_3Sn . Only a trace amount of ethane was observed after 100 min of reaction. In the case of Ni_3Sn_2 , ethane was not observed even after 120 min. When the reaction was carried out on nickel at the same temperature (523 K), ethane was still the final product. It is shown that Ni_3Sn and Ni_3Sn_2 catalysts have a high selectivity for the partial hydrogenation of acetylene into ethylene. In the case of acetylene hydrogenation on Co–Ge IMC, we have reported that CoGe showed the higher selectivity into ethylene.²⁴ The cause of partial hydrogenation would be either the deactivation by coke or the intrinsic properties of Ni–Sn IMCs. After evacuating the used Ni–Sn IMC catalyst at 523 K, the acetylene hydrogenation was carried out again. The results on the second run were quite similar to those on the first run. This indicates that the partial hydrogenation into ethylene was not caused by the rapid deactivation by coke.

Hydrocarbons with carbon number of four and higher (C_{4+}) were also formed in addition to ethylene and ethane in Fig. 6. The fraction of C_{4+} did not increase after acetylene was completely converted. Over pure nickel, C_{4+} contained mainly butane after 20 min of the reaction. Butane would be the hydrogenation product of an acetylene dimer. Over Ni_3Sn and Ni_3Sn_2 , C_{4+} hydrocarbons were also formed. After 90 min of the reaction, most of the C_{4+} hydrocarbons were butenes over Ni_3Sn and 1,3-butadiene over Ni_3Sn_2 . The selectivity in the secondary hydrogenation of C_4 hydrocarbon products was also specific to Ni–Sn IMCs.

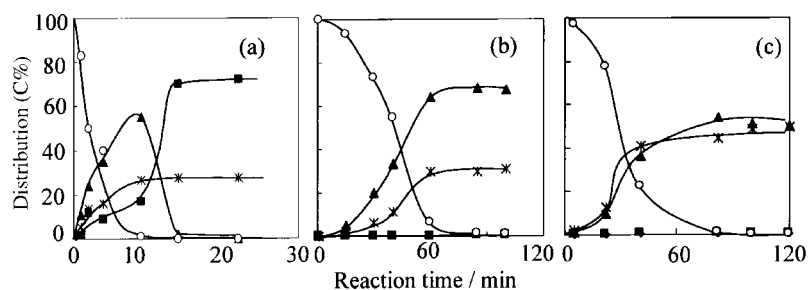


Fig. 6 Change in gas phase composition of hydrocarbons during the hydrogenation of acetylene over pure nickel (a, 0.30 g) at 373 K, Ni_3Sn (b, 0.30 g) and Ni_3Sn_2 (c, 0.50 g) at 523 K. $P(H_2) = 13$ kPa, $P(C_2H_2) = 2.7$ kPa. ○: acetylene, ▲: ethylene, ■: ethane, ×: C_{4+} .

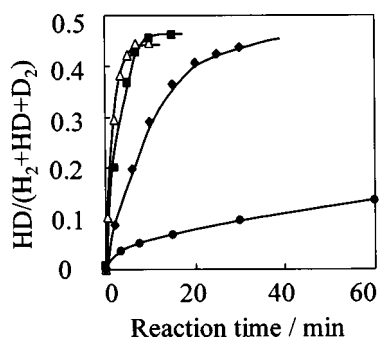


Fig. 7 H_2 - D_2 equilibration over nickel (Δ , 0.10 g) at 373 K, Ni_3Sn (\blacksquare , 0.10 g), Ni_3Sn_2 (\blacklozenge , 0.50 g) and Ni_3Sn_4 (\bullet , 0.50 g) at 523 K. $P(H_2) = P(D_2) = 6.7$ kPa.

In order to clarify the cause of these catalytic phenomena, firstly we will discuss the activity of Ni-Sn IMCs for the acetylene hydrogenation. The kinetic measurements over nickel, Ni_3Sn and Ni_3Sn_2 revealed that the rate of acetylene hydrogenation did not depend on the partial pressure of acetylene but depended positively on that of hydrogen. The rate-limiting step would be the dissociation of hydrogen. Therefore, the H_2 - D_2 equilibration was carried out to clarify the abilities of Ni-Sn IMCs for the dissociative adsorption of hydrogen. The reactions were carried out at the same temperatures as acetylene hydrogenation, that is, 523 K over Ni-Sn IMCs and 373 K over nickel. Catalysts were pretreated with hydrogen at 873 K for 1 h. Fig. 7 shows the change in the fraction of HD as a fraction of reaction time. HD was formed readily at 373 K over pure nickel. The HD fraction was leveled at about 47%, which is close to its equilibrium value, 47.5% at 373 K. No formation of HD was observed over Ni_3Sn at 373 K. Ni_3Sn showed almost a similar rate of HD formation at 523 K to that over nickel at 373 K. Ni_3Sn_2 (0.50 g) exhibited a lower HD formation rate than Ni_3Sn (0.10 g). The fraction of HD on Ni_3Sn and Ni_3Sn_2 approached its equilibrium value, 48.7% at 523 K. Ni_3Sn_4 also exhibited an activity for the H_2 - D_2 equilibration, in spite of the inactivity for the hydrogenation of acetylene (see Fig. 5).

Table 2 shows the initial rate of HD formation and acetylene conversion per weight of catalysts together with the surface nickel concentration measured by XPS. The orders of the rates of the HD formation and acetylene hydrogenation are the same as that of the nickel concentration near surface, that is nickel > Ni_3Sn > Ni_3Sn_2 > Ni_3Sn_4 . However, the differences in reaction rates among these catalysts were much larger than those in the nickel concentrations. Especially, there was a large difference in activity between pure nickel and Ni-Sn IMCs, because the reaction temperature for pure nickel was 150 K lower than that for Ni-Sn IMCs. Therefore, the number of surface nickel atoms does not account for the larger difference in catalytic activities. There would be electronic or geometric effects on the active site for H_2 - D_2 equilibration.

It was reported by Satoko *et al.* that hydrogen molecules would dissociate on an on-top site of a nickel from the LCAO- $A\alpha$ energy gradient model.³⁶ Their result would suggest that the activity for the dissociation of hydrogen and

the H_2 - D_2 equilibration depends mainly on electron density of active atoms but not on the distance between the active atoms. The dissociation of hydrogen is induced by the back donation, that is the electron transfer, from Ni3d to the hydrogen molecule. In this study, the electron density of surface nickel atoms corresponds to the valence band at the Fermi level. As shown in Fig. 4, the increase in tin concentration led to the decrease in electron density at the Fermi level from 1170 (Ni) to 430 cps (Ni_3Sn_4). This decrease in electron density will suppress the activity for the hydrogen dissociation. The nickel atoms on Ni_3Sn_4 have activity for the dissociation of hydrogen but their distance might be too long to activate acetylene.

We will now discuss the selectivity for the partial hydrogenation of acetylene into ethylene over Ni-Sn IMCs. Over pure nickel and Ni-Sn IMC catalysts, ethylene hydrogenation was carried out under the same reaction conditions as those in acetylene hydrogenation. Fig. 8 compares the change in total pressure for acetylene and ethylene hydrogenation over nickel (a), Ni_3Sn (b) and Ni_3Sn_2 (c). Ni_3Sn_4 did not catalyze ethylene hydrogenation or acetylene hydrogenation. Over nickel, the rate of ethylene hydrogenation was much faster than that of acetylene hydrogenation. Acetylene would be adsorbed on the nickel surface more strongly than ethylene and most of the active sites for hydrogen dissociation would be covered with acetylene during acetylene hydrogenation.²⁶

Fig. 8c shows that over Ni_3Sn_2 ethylene hydrogenation did not proceed at 523 K, though acetylene hydrogenation proceeded significantly. These results are in marked contrast with those of nickel (a). Ethane was not detected in ethylene hydrogenation even at higher temperatures, 523–723 K. It is clarified that the partial hydrogenation of acetylene on Ni_3Sn_2 is caused by the lack of activity for ethylene hydrogenation. In the case of the Ni_3Sn catalyst, ethylene was significantly hydrogenated into ethane as shown in Fig. 8b. However, during the acetylene hydrogenation, the formation of ethane was scarcely observed (Fig. 6b). There may be a few sites for ethylene hydrogenation of Ni_3Sn surface. These sites would be easily poisoned by coke from acetylene in acetylene hydrogenation. In fact, ethylene hydrogenation did not proceed over Ni_3Sn which had been used for acetylene hydrogenation and then evacuated at 523 K.

Fig. 9 shows the H_2 - D_2 equilibration in the presence of acetylene or ethylene at 523 K on Ni_3Sn (a) and Ni_3Sn_2 (b). The rate of H_2 - D_2 equilibration with acetylene over Ni_3Sn_2 was much lower than that without hydrocarbon, which indicates the inhibition of the dissociative adsorption of hydrogen by the adsorbed acetylene species. This result is consistent with the lower rate of acetylene hydrogenation to that of H_2 - D_2 equilibration (Table 2). On the other hand, the rate of H_2 - D_2 equilibration with ethylene over Ni_3Sn_2 was almost the same as that without hydrocarbon. These results imply that the active sites for hydrogen dissociation are blocked not by ethylene but by acetylene. The strength of adsorption on Ni_3Sn_2 would be the following order,



In the case of Ni_3Sn (Fig. 9a), the rate of H_2 - D_2 equilibration with ethylene was slightly lower than that without

Table 2 Initial rate of acetylene hydrogenation and H_2 - D_2 equilibration

| Catalyst (reaction temp.) | Acetylene conversion / 10^{-6} mol s $^{-1}$ g $^{-1}$ | HD formation / 10^{-6} mol s $^{-1}$ g $^{-1}$ | Surface nickel composition ^a (atom%) |
|---------------------------|--|--|---|
| Ni (373 K) | 2.8 | 45 | 100 |
| Ni_3Sn (523 K) | 2.3 | 30 | 57 |
| Ni_3Sn_2 (523 K) | 0.6 | 2.6 | 42 |
| Ni_3Sn_4 (523 K) | <0.001 | 0.59 | 28 |

^a Determined by XPS.

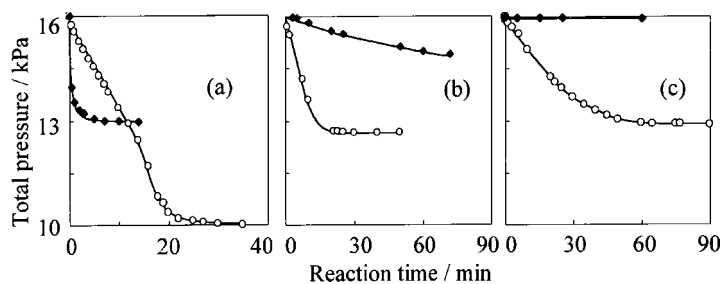
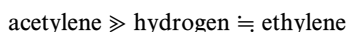


Fig. 8 Comparison of the hydrogenation of acetylene (O) and ethylene (◆) over pure nickel (a, 0.30 g) at 373 K, Ni₃Sn (b, 0.30 g) and Ni₃Sn₂ (c, 0.50 g) at 523 K. $P(\text{H}_2) = 13 \text{ kPa}$, $P(\text{C}_2\text{H}_2) = P(\text{C}_2\text{H}_4) = 2.7 \text{ kPa}$.

hydrocarbon. With acetylene, the initial rate was much lower. The strength of adsorption on Ni₃Sn would be the following order;



After complete conversion of acetylene in 40 min, the reaction rate increased to approach the rate with ethylene. As mentioned above, the active sites on Ni₃Sn for ethylene hydrogenation were poisoned during acetylene hydrogenation, while those for acetylene hydrogenation were scarcely poisoned. There would be quite a few active sites for ethylene hydrogenation on the surface of Ni₃Sn. In addition, this order of adsorption would be consistent with the kinetic results, that is, the rate of ethylene hydrogenation was 0.9th order in hydrogen and 0.8th order in ethylene. In conclusion, because the adsorption of ethylene is very weak on Ni₃Sn and Ni₃Sn₂, the rate of ethylene hydrogenation is much lower than that of acetylene hydrogenation over Ni₃Sn and ethylene hydrogenation did not proceed over Ni₃Sn₂.

To clarify further the interaction of Ni–Sn IMCs with ethylene, the H–D exchange between C₂D₄ and H₂ was studied over Ni₃Sn and Ni₃Sn₂. Fig. 10 shows the change in the gas

phase distribution of hydrocarbons over Ni₃Sn (a) and Ni₃Sn₂ (b) at 523 K. Over Ni₃Sn₂, C₂D₄ molecules ($m/z = 32$) were converted into C₂D₃H ($m/z = 31$), because ethylene was not hydrogenated into ethane over Ni₃Sn₂. It is clear that Ni₃Sn₂ catalyzed H–D exchange between ethylene and hydrogen although it has no hydrogenating activity for ethylene. Ni₃Sn (a) rapidly converted C₂D₄ into products with $m/z = 28, 29, 30, 31, 32, 33\text{--}36$. At 20 min of reaction, most of the products with m/z less than 32 (C₂D₄) would be ethylene, because Ni₃Sn converted only 10% of ethylene into ethane over 20 min (Fig. 8b). The H–D exchange in ethylene reached the equilibrium within 20 min. It is clear that the rate of H–D exchange is much faster than that of ethylene hydrogenation over Ni₃Sn. The equilibration of C₂D₄–C₂H₄ also proceeded on Ni₃Sn and Ni₃Sn₂ at the same reaction temperature. These results would mean that the H–D exchange between C₂D₄ and H₂ on Ni₃Sn and Ni₃Sn₂ does not proceed through the Rideal–Eley mechanism but through the Langmuir–Hinshelwood mechanism with ethylene chemisorbed on the surface. It is concluded that the adsorbed species of ethylene exist on Ni₃Sn and Ni₃Sn₂ during ethylene hydrogenation.

We will now discuss a reaction intermediate for the H–D exchange between C₂D₄ and H₂ on Ni₃Sn₂. The intermediate would be ethyl species (7) or vinyl species (2) in Scheme 1 which was drawn based on the report by Margitfalvi *et al.* on palladium brack.³⁷ We considered that the intermediate adsorbed on Ni₃Sn₂ would not be the ethyl species that the vinyl species. If the ethyl species were present, they would be

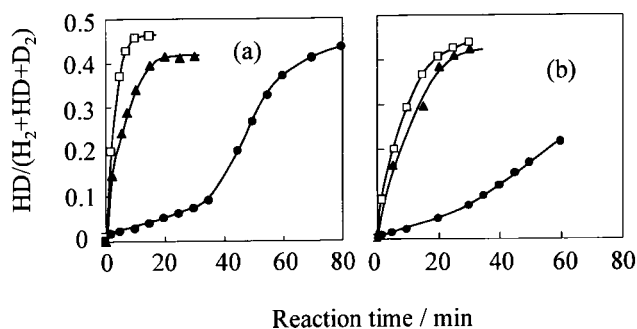


Fig. 9 H₂–D₂ equilibration without hydrocarbon (□), with ethylene (▲) and with acetylene (●) on Ni₃Sn (a, 0.10 g) and Ni₃Sn₂ (b, 0.50 g) at 523 K. $P(\text{H}_2) = P(\text{D}_2) = 6.7 \text{ kPa}$, $P(\text{C}_2\text{H}_2) = P(\text{C}_2\text{H}_4) = 2.7 \text{ kPa}$.

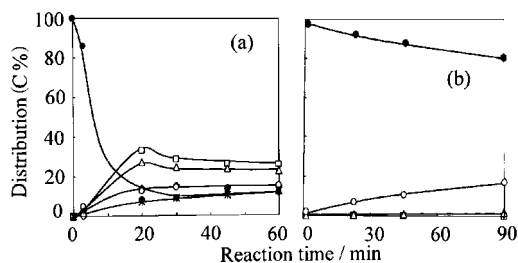
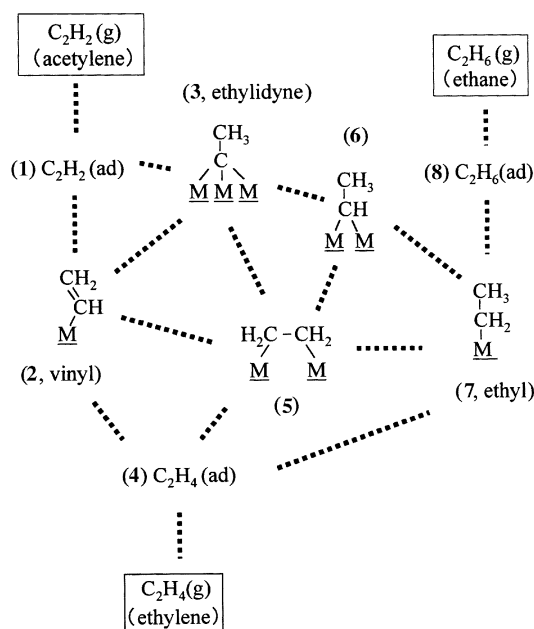


Fig. 10 H–D exchange between C₂D₄ and H₂ over Ni₃Sn (a, 0.30 g) and Ni₃Sn₂ (b, 0.50 g) at 523 K. $P(\text{C}_2\text{D}_4) = 2.7 \text{ kPa}$, $P(\text{H}_2) = 1.3 \text{ kPa}$.
 ◇: $m/z = 28$: C₂H₄, □: 29: C₂H₃D, △: 30: C₂H₂D₂ + C₂H₆,
 ○: 31: C₂HD₃ + C₂H₃D, ●: 32: C₂D₄ + C₂H₄D₂,
 ✱: 33–36: C₂H₃D₃ + C₂H₂D₄ + C₂HD₅ + C₂D₆.



Scheme 1 Possible reaction scheme for the hydrogenation of ethylene and acetylene.

hydrogenated into ethane at higher temperatures. However, ethane was not detected in ethylene hydrogenation even at 723 K. In addition, the vinyl species will be formed from ethylene on Ni_3Sn_2 because the vinyl species must be the intermediate for the acetylene hydrogenation into ethylene. The formation of vinyl species from ethylene has already been reported on nickel.³⁸ It would be then deduced that the inhibition of ethylene hydrogenation is owing to the absence of ethyl species on Ni_3Sn_2 .

Next, we will discuss why the ethyl species are not formed on Ni_3Sn_2 . We assumed that the major reason for the absence of ethyl species is not the electronic effect of tin but the geometric restriction on the adsorption sites because ethane was not detected in ethylene hydrogenation even at higher temperature of 723 K. From the geometric point of view, the most strongly restricted species in Scheme 1 will be ethylidyne³⁹ species (3). It was reported that ethylidyne was not hydrogenated below 300 K over platinum and weakly adsorbed ethylene would be the intermediates for the ethylene hydrogenation (4 → 7).^{40–41} We suggested that, at least above 523 K, ethylidyne is the significant species for the ethylene hydrogenation and would be one of the intermediates for the hydrogenation into ethane and that the absence of the ethyl species on Ni_3Sn_2 is caused by the absence of ethylidyne species.

Thus, the geometric restriction on the ethylidyne formation was presumed to be the cause of the high selectivity for the partial hydrogenation of acetylene into ethylene over Ni_3Sn_2 . The same discussion might be applied to Ni_3Sn . However, it is necessary to consider that the electronic effect may be a cause of the inhibition of ethylene hydrogenation on Ni_3Sn_2 whose electron density at Fermi level was clarified to be less than that of nickel according to XPS.

4. Conclusions

TPR revealed that the surfaces of pure nickel, Ni_3Sn , Ni_3Sn_2 and Ni_3Sn_4 intermetallic compounds (IMCs) have individual reduction behaviors. XPS identified the following three facts. The surface nickel and tin atoms of these IMCs are in metallic states after the pretreatment with hydrogen at 873 K. The nickel composition near the surface increases with the increase in that in the bulk. The electron transfer from tin to nickel increases with the increase in tin composition. These characterizations clarified that Ni_3Sn , Ni_3Sn_2 and Ni_3Sn_4 each have the genuine surface of an intermetallic phase.

Each Ni–Sn IMC has specific catalytic properties different from pure nickel and the other Ni–Sn IMCs for the hydrogenation of acetylene and ethylene, H_2 – D_2 equilibration and H–D exchange between deuterated ethylene and hydrogen. The order of activity for acetylene hydrogenation is $\text{Ni} \gg \text{Ni}_3\text{Sn} > \text{Ni}_3\text{Sn}_2 \gg \text{Ni}_3\text{Sn}_4$. This activity should depend on the activity for hydrogen dissociation. The difference in activity is much larger than the difference in the number of surface nickel atoms and would be related to the difference in electron density of nickel valence band at Fermi level. Ni_3Sn shows the high selectivity into ethylene in acetylene hydrogenation and has a small amount of active sites for ethylene hydrogenation. Ni_3Sn_2 also catalyzes the partial hydrogenation of acetylene into ethylene but does not catalyze the ethylene hydrogenation. Ni_3Sn_4 has the active site not for the hydrogenation of acetylene and ethylene but for the dissociation of hydrogen. It is presumed that the inhibition of ethylene hydrogenation over Ni_3Sn_2 is due to the absence of ethylidyne species by geometric restriction.

References

- W. E. Wallace, *CHEMTECH*, 1982, **12**, 752.
- T. Takeshi, W. E. Wallace and R. S. Craig, *J. Catal.*, 1976, **44**, 236.
- K. Soga, H. Imamura and S. Ikeda, *J. Phys. Chem.*, 1977, **81**, 1762.
- A. P. Walker, T. Rayment and R. M. Lambert, *J. Catal.*, 1989, **117**, 102.
- V. T. Coon, T. Takeshita, W. E. Wallace and R. S. Crag, *J. Phys. Chem.*, 1976, **80**, 1878.
- A. Elattar, T. Takeshita, W. E. Wallace and R. S. Crag, *Science*, 1977, **80**, 1093.
- C. A. Luengo, A. L. Cabrera, H. B. Mackey and M. B. Mayple, *J. Catal.*, 1977, **47**, 1.
- H. Imamura and W. E. Wallace, *J. Phys. Chem.*, 1980, **84**, 3145.
- R. Sasikala, N. M. Gupta, S. K. Kulshreththa and R. M. Iyer, *J. Catal.*, 1987, **107**, 510.
- A. Bahia and J. M. Winterbottom, *J. Chem. Tech. Biotechnol.*, 1994, **60**, 305.
- T. P. Chojnacki and L. D. Schmidt, *J. Catal.*, 1991, **129**, 473.
- J. H. Sinfelt, *Bimetallic Catalysts: Discoveries, Concepts and Applications*, Wiley, New York, 1983.
- C. Kappenstein, M. Guerin, K. Lazar, K. Matusek and Z. Paal, *J. Chem. Soc., Faraday Trans.*, 1998, **94**, 2463.
- S. T. Srinivas and P. K. Rao, *J. Catal.*, 1998, **179**, 1.
- Z. Huang, J. R. Fryer, C. Park, D. Stirling and G. Webb, *J. Catal.*, 1996, **159**, 340.
- F. M. Dautzenberg, J. N. Helle, P. Biloen and M. H. Sachtler, *J. Catal.*, 1980, **63**, 119.
- J. Llorca, P. R. de la Piscina, J.-L. G. Fierro, J. Sales and N. Homs, *J. Catal.*, 1995, **156**, 139.
- M. Masai, K. Mori, H. Muramoto, T. Fujiwara and S. Ohnaka, *J. Catal.*, 1975, **38**, 128.
- M. Masai, K. Mori, H. Muramoto, T. Fujiwara and S. Ohnaka, *J. Catal.*, 1977, **50**, 419.
- H. Verbeeck and W. M. H. Sachtler, *J. Catal.*, 1976, **42**, 257.
- P. M. Holmblad, J. H. Larsen, I. Chorkedorff, R. P. Nielsen, F. Besenbacher, I. Stensgaard, E. Lægsgaard, P. Kratzer, B. Hammer and J. K. Nørkov, *Catal. Lett.*, 1996, **40**, 131.
- M. T. Paffett, S. C. Gebhard, R. G. Windham and B. E. Koel, *Surf. Sci.*, 1989, **223**, 449.
- Y. K. Park, F. H. Ribeiro and G. A. Somorjai, *J. Catal.*, 1998, **178**, 66.
- T. Komatsu, M. Fukui and T. Yashima, '11th Intern. Congr. Catal.—40th Anniversary', *Stud. Surf. Sci. Catal.*, 1996, **101**, 1095.
- T. Komatsu, S. Hyodo and T. Yashima, *J. Phys. Chem. B*, 1996, **101**, 5565.
- G. C. Bond, *Catalysis by Metals*, Academic Press, London and New York, 1962.
- T. B. Massalski, H. Okamoto, P. R. Subramanian and L. Kacprzak, *Binary Alloy Phase Diagrams, Second Edition*, ASM International and National Institute of Standard and Technology, 1990.
- G. E. Moulder, W. F. Stickle, P. E. Sobol and K. D. Bomben, *Handbook of X-ray Photoelectron Spectroscopy*, Perkin-Elmer Corporation, Physical Electronics Division, 2nd edn., 1992.
- C. D. Wagner, L. E. Davis, M. V. Zeller, J. A. Taylor, R. A. Raymond and L. H. Gale, *SIA Surf. Interface Anal.*, 1981, **3**, 211.
- F. U. Hillebrecht, J. C. Fuggle, P. A. Bannet, Z. Zolnierec and C. Freiburg, *Phys. Rev. B*, 1982, **27**, 2179.
- R. A. Miedema, *Z. Metallkol.*, 1978, **69**, 287.
- S. K. Overbury, P. A. Bertrant and G. A. Somorjai, *Chem. Rev.*, 1975, **75**, 547.
- J. C. Fuggle, F. U. Hillebrecht, R. Zeller, Z. Zolnierec, P. A. Bannet and C. Freiburg, *Phys. Rev. Sect. B*, 1982, **27**, 2145.
- C. S. Fadley and D. A. Shirley, *J. Res. Natl. Bur. Stand., Sect. A*, 1970, **74**, 543.
- S. Hufner, G. K. Wertheim, R. L. Cohen and J. H. Wernick, *Phys. Rev. Lett.*, 1972, **28**, 488.
- S. Satoko and M. Tsukada, *Surf. Sci.*, 1983, **134**, 1.
- J. Margitfalvi, L. Guzzi and A. H. Weiss, *React. Kinet. Catal. Lett.*, 1980, **15**(4), 475.
- O. Beeck, *Adv. Catal.*, 1950, **2**, 151.
- M. P. Lapinski and J. G. Ekerdt, *J. Phys. Chem.*, 1988, **92**, 1709.
- S. M. Davis, F. Zaera, B. E. Gordon and G. A. Somorjai, *J. Catal.*, 1985, **92**, 240.
- P. S. Cremer, X. Su, Y. R. Shen and G. A. Somorjai, *Catal. Lett.*, 1996, **40**, 143.